

A VIRTUAL TEST LAB FOR UNIDIRECTIONAL COMPOSITE COUPONS

Olben Falcó¹, Bas Tijss², Brendan Romano², Cláudio S. Lopes¹

¹IMDEA Materials, Getafe, Madrid, Spain

Email: claudiosaul.lopes@imdea.org, Web Page: <https://materials.imdea.org>

²GKN Aerospace: Fokker, Papendrecht, The Netherlands

Email: bas.tijss@fokker.com, Web Page: <http://www.fokker.com>

Keywords: Progressive Failure Analyses (PFA); Finite Element Analyses (FEA); open-hole; low-velocity impact; compression-after-impact; bolt-bearing.

Abstract

A reliable virtual testing framework for unidirectional laminated composites is presented that allows the prediction of failure loads and modes of general in-plane coupons with great realism. This is a toolset based on mesomechanical finite element analysis that relies on a cohesive-frictional constitutive formulation coupled with the kinematics of penalty-based contact surfaces, on a sophisticated three-dimensional continuum damage model, and overall on a modelling approach based on mesh structuring and crack-band erosion to capture the appropriate crack paths in unidirectional fibre reinforced plies. An extensive and rigorous validation of the overall approach is presented, demonstrating that the virtual testing laboratory is robust and can be reliably used in for composite materials screening, design and certification.

1. Introduction

Although accurate numerical approaches have been proposed to simulate particular laminate configurations, there is yet no efficient and reliable numerical framework for general virtual testing of composites coupons, including the multiple test standard used for material certification. This paper presents an efficient and robust virtual testing toolset to perform reliable simulation of unidirectional composite laminated coupons that predicts competing ply and interface damage mechanisms and, overall, laminate failure modes with great realism. This virtual test framework consists of several tools, namely: i) a commercially-available explicit FE solver tool (ABAQUS/Explicit [1]) to tackle the numerous sources of nonlinearities in the models in an efficient way; ii) a sophisticated three-dimensional CDM for unidirectional FRP plies, implemented by means of a user subroutine in the FE solver, that enforces element erosion; iii) a surface-based cohesive-frictional numerical approach to model ply interfaces; iv) a purpose-built automated ABAQUS plug-in, based on Python code, for the meso-modelling of unidirectional laminated coupons that applies regularized meshes, i.e. controlled mesh size, mesh-alignment and directional biasing, in this way enforcing damage localization along physically-sound crack paths.

This work demonstrates that the sound kinematic simulation of composite damage modes and the accurate prediction of failure loads can be achieved by combining conventional constitutive approaches with appropriate discretization and meshing of ply and interfaces. An extensive validation of the virtual testing toolset is presented for notched/unnotched coupon testing, bolt bearing, low-velocity impact and compression-after-impact.

2. Virtual Test Laboratory

The explicit FE method implemented in ABAQUS/Explicit [1] was the computational framework selected to carry the highly nonlinear dynamic problems which would cause convergence difficulties to implicit integration procedures. A dedicated ABAQUS plug-in was built on purpose for the meso-modelling of unidirectional FRP coupons according to the presented approach. The numerical tool, which allows modelling of coupons with conventional and nonconventional ply angles, has been implemented by means of the programming language Python using ABAQUS scripting commands [1]

and includes a Graphical User Interface (GUI). This tool is completely automated without the need for the use of any third-party software or manual intervention, except for the introduction of model inputs.

2.1. Constitutive models for plies and interfaces

The unidirectional FRP plies are modelled by means of a thermodynamically-consistent CDM, based on the work of Maimí et al. [2,3], that guarantees the appropriate energy dissipation for different physically-observed fracture modes. Important modifications were introduced to improve the constitutive representation. The original plane-stress formulation was extended to take into account three-dimensional stress states. Nonlinear elastic-plastic behaviours were adopted for in-plane and out-of-plane shear responses based on Ramberg-Osgood laws [4]. First-ply failure is detected by means of physically-based three-dimensional failure criteria proposed by Catalanotti et al. [5]. The gradual unloading of a ply after the onset of damage is simulated according to different damage evolution laws in different orthotropic directions associated with damage variables d_M corresponding to damage modes: longitudinal tension/compression ($M=1\pm$); transverse tension/compression ($M=2\pm$); out-of-plane transverse shear ($M=4$); out-of-plane longitudinal shear ($M=5$) and in-plane shear ($M=6$) directions. All out-of-plane damage mechanisms in the laminate are considered to be lumped into possible interface delamination, hence, out-of-plane ply softening is prevented ($d_3=0$). Exponential damage laws are used to model material softening corresponding to the damage processes of fibre kinking and matrix cracking. To simulate ply failure under longitudinal tensile loads, a coupled linear-exponential softening law is used to model separately the mechanisms of fibre breakage and fibre pull-out [2,3]. In this work, the parameters of this softening law are derived from the analysis of the experimentally-obtained crack resistance curve (R-curve) by applying the data reduction method proposed by Dávila et al. [6]. Moreover, matrix cracking is assumed to occur under general mixed-mode conditions, with onset load and fracture angle predicted by the maximization of quadratic-interactive three-dimensional failure criteria [5]. The propagation of matrix cracking is determined by the energy-based Benzeggagh-Kenane (BK) criterion [7] that accounts for the dependence of the fracture energy dissipation on the mode mixity ratio.

Zero-thickness ply interfaces are modelled by means of a surface-based cohesive-frictional formulation coupled to penalty contact behavior between the plies. This approach is implemented in the kinematics of surface contact interaction algorithms available in ABAQUS/Explicit [1]. The coupled cohesive-frictional approach is adopted to include the possible effects of ply friction during and after delamination. In this way, the shear stresses caused by friction at the interface are ramped progressively and proportional to the degradation of the interface, thus once the interface is fully delaminated, the surface interaction is uniquely governed by a pure Coulomb friction model. For the pure cohesive response, damage onset is identified by means of a quadratic interaction criterion that is a function of the interlaminar strength values for each of the damage modes. Once delamination is initiated, the cohesive tractions transferred through the interface decrease linearly to zero dissipating the fracture energy corresponding to the specific mixed-mode loading mode, as given by the BK damage propagation criterion [7]. The interface fracture properties are assumed to be dependent on the interface mismatch angle [8].

2.2. Modelling techniques for unidirectional FRP coupons

The laminated FRP specimen with the desired stacking sequence is assembled from several parts (see Figure 1). The coupons are divided in three zones with two different levels of discretization in order to minimize the necessary computational resources and ensure the localization of failure mechanisms in the central section of the specimens. In this section, each ply is discretized with a structured material-aligned meshing technique, with a refined layer of reduced integration solid elements (C3D8R in ABAQUS [1]), facilitated by a purpose-built mesh generation algorithm [8]. The discretized plies behave according to the constitutive model for unidirectional composite materials introduced above, which has been coded in a double-precision Fortran-written user material subroutine 'VUMAT'. The ply interface behaviour is taken into account by means of the ABAQUS-native surface-based cohesive-frictional interactions that facilitate the use of non-conformal ply meshes, hence allowing the use of mesh alignment, mesh directional biasing and different element sizes in different plies. To allow

the correct dissipation of the fracture energy while preventing snap-back behaviour in the constitutive relations, the element in-plane characteristic dimensions on each ply are constrained by maximum values which are function of the ply 'in-situ' properties [8].

Away from the centre, around the load application edges, the orthotropic layers are assumed to behave elastically and are modelled by coarse solid-like continuum shell elements with one integration point per ply. The three regions with different discretizations are kinematically constrained to enforce continuity of displacements and rotations across their boundaries. Specially in the cases of un-notched coupons, the damage zone is guaranteed to be long enough to represent ply and interface damage accumulation before their final failure. In order to avoid spurious damage due to unrealistic stress oscillations, stress softening is prevented in plies and interfaces in smooth transition zones close to the regions of kinematic constraining. For symmetric layups, symmetry boundary conditions are applied on the mid-plane of the virtual specimen.

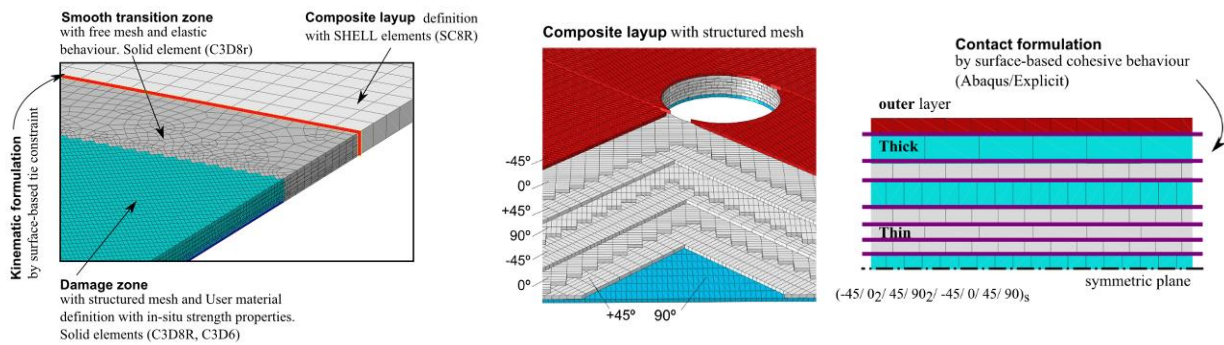


Figure 1. Schematics of the general coupon modelling approach

2.3. Mesh regularization: size, alignment and biasing

The mesh regularization scheme proposed by Bažant and Oh [9] is employed to assure energy-objective solutions. Another source of mesh-dependence in strain-localization models is mesh-induced direction bias. The misalignment between crack band direction and mesh lines induces stresses locking because of the continuity in displacement of the FE method [10]. In unidirectional composites, microstructure dictates that matrix cracks develop along the longitudinal direction while fibre breakage and kinking tend to occur transverse to it. Therefore, a practical solution to mitigate mesh-induced directional bias in these materials consists in the alignment of mesh lines with orthotropic material directions, as demonstrated in [8]. Moreover, to simulate the correct physical propagation of transverse cracks in unidirectional FRP, mesh-alignment is not sufficient. In addition, a large element aspect ratio (in longitudinal to transverse material directions) is needed to prevent the crack from deviating from its microstructure-allowed path. This increase of the element aspect ratio represents a directional biasing of the degrees of freedom (DOF) available in the model that prevents crack deviation from their microstructure-constrained path.

2.4. Crack-band erosion

An advantage of using material-aligned meshes is that it facilitates the use of element erosion to simulate material cracks in the strong sense. i.e. with kinematic discontinuities between crack faces [8]. Once an element is removed from the mesh, penalty-based frictional contact conditions are enforced at the free faces of the neighbouring elements to model the crack faces, avoiding interpenetration and allowing stress transfer in case of crack closure. A second motivation for element erosion is the avoidance of excessive element distortions that would condition the efficiency of the simulations and compromise the accuracy of the numerical solutions.

3. Demonstration and validation

Several coupon test cases typically used for the purpose of certification of composite materials in aeronautics are selected herein to validate the virtual test laboratory: in-plane un-notched tension/compression (UNT/UNC), open-hole tension/compression (OHT/OHC), bolt bearing, low

velocity impact (LVI) and compression-after-impact (CAI). All laminates are made of unidirectional AS4/8552 plies whose properties, together with ply-interface behaviour parameters, are reported in [8]. A thermal analysis step is conducted prior to the application of mechanical loading, in order to simulate the influence of thermal residual stress resulting from curing cool-down. Except for impact cases, mass scaling is used (up to 1000x) to increase the explicit analysis stable time increment to practical levels, improving the computation time. These conditions ensure the quasi-static nature of coupon deformation which is guaranteed by keeping the specimen kinetic at a level two orders of magnitude lower than its internal energy and by observing that there are no dynamic oscillations in the load-displacement results.

3.1. Plain and open-hole strengths

Virtual tension and compression tests were performed on UNT/UNC and OHT/OHC coupons of three different laminate configurations previously analysed by Fokker and the National Center for Advanced Materials Performance (NCAMP) [11] through independent extensive experimental campaigns intended to provide material design allowable values for laminate configurations commonly used to design and certify aircraft structures, and to fulfil base material qualification requirements [11]. The configurations constitute limits of the design space in terms of stiffness properties. This is reflected in the following percentage ratios of plies in the 0°, ±45°, and 90° directions: 50/40/10 (fibre-dominated or 'hard'); 25/50/25 (QI); and 10/80/10 (transversely dominated or 'soft'). The corresponding stacking sequences are, respectively, [0/45/0/90/0/-45/0/45/0/-45]_s, [-45/0/45/90]_{2s} and [45/-45/0/45/-45/90/45/-45/45/-45]_s. The experimental and simulated results are represented in Figure 2.

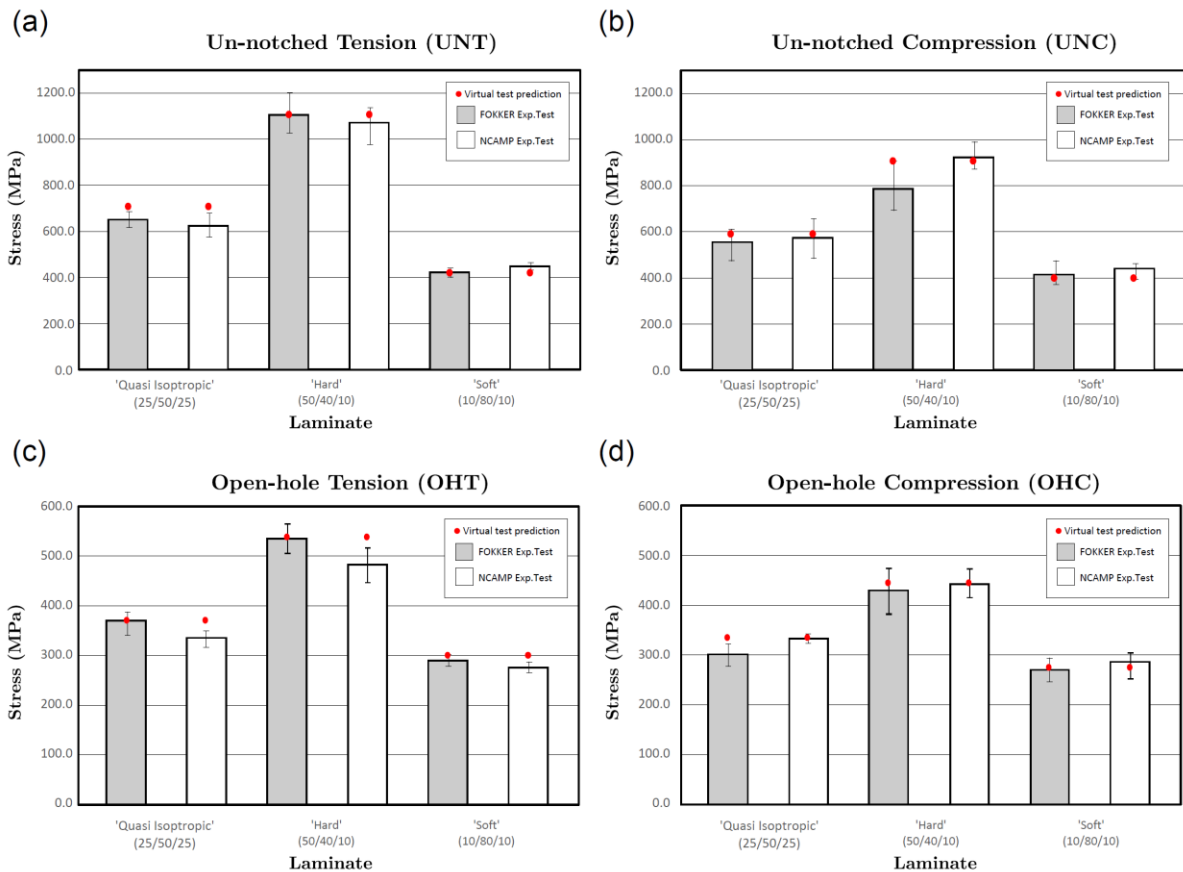


Figure 2. Correlation between experimental and virtual test results of a) UNT, b)UNC, c) OHT and d) OHC coupons [8] (minimum and maximum experimental values obtained for each test configuration are indicated).

The experimental tensile test results obtained by Fokker are systematically higher than the ones from NCAMP, reflecting the differences in material batch (and processing conditions). On the other hand, for compression tests, Fokker values are systematically lower than NCAMP's, as result of different

material batches and test conditions. In general lines, the tensile virtual test results fall within the scatter of Fokker's experimental results while compression test simulations correlate better with NCAMP's experimental scatter. In general, the simulation predictions are within a 10% deviation from experimental values.

Distinct final failure mechanisms were observed for distinct configurations, and these were remarkably captured by the simulations [8]. While for the unnotched coupons the global failure mode was brittle, a progressive failure behaviour with interacting ply and interface failure mechanisms was observed in the open-hole specimens, with damage initiating around the hole and free edges, and propagating towards the inner sections. As an example, the simulation on the 'soft' (10/80/10) OHT coupon is illustrated in Figure 3.

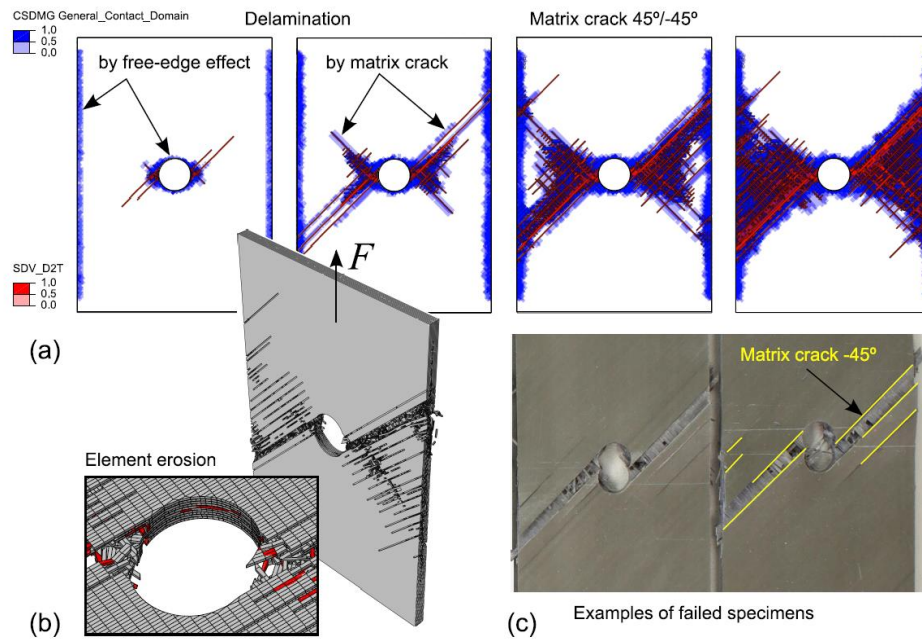


Figure 3. Experimentally-observed (c) and simulated (a; b) progression of failure mechanisms in OHT specimens of 'soft' laminates (10/80/10): (a) undeformed damage evolution of delamination and matrix cracking. (b) realistic transverse cracks simulated by means of crack-band erosion. (c) experimentally-observed failure modes in failed specimens (photo: Fokker).

3.2. Bolt bearing

Bearing failure is a local compressive failure mode due to contact and frictional forces acting on the surface of the hole. This fracture process is influenced by many parameters, including laminate thickness, hole diameter, width/diameter and edge/diameter ratios, stacking sequence, ply orientation, coefficient of friction, lateral constraining and clamping force, radial clearance between bolt and specimen, and washer dimensions [12,13]. These effects can be simulated in the developed Virtual Test Lab. To this end, the AIRBUS standard bolt bearing test method AITM 1-0009 [14] on a quasi-isotropic $[\pm 45/0/90/0/\pm 45/90]_s$ AS4/8552 laminate was modelled, as represented in Figure 4.

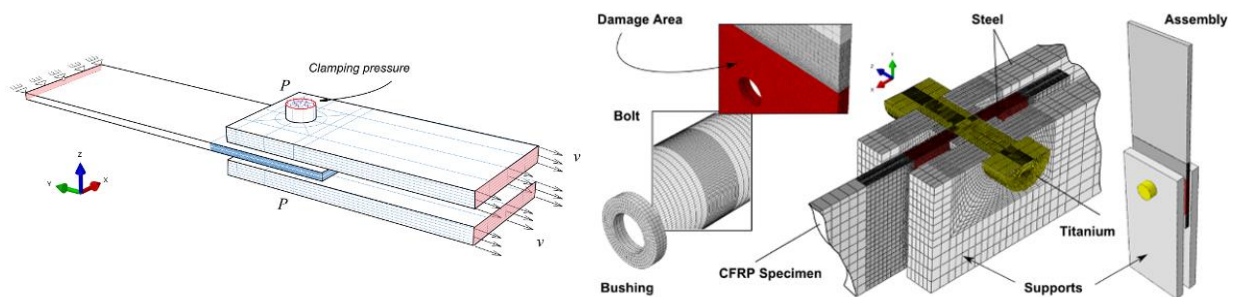


Figure 4. Schematics of the modelling approach of the bolt bearing test (AITM 1-0009).

The simulated bolt bearing stress vs. hole deformation curve is represented in Figure 5. The loading curve starts with an approximately linear region and whose slope represents the initial elastic stiffness of the specimen. The non-linearity in the load response is caused by the damage accumulated in specimen bearing and the resulting hole elongation. The offset bearing strength was calculated at the intersection of the dashed ‘Offset Stiffness Lines’ at 0.5%, 2.0%, 4.0% and 6.0% hole deformation with the load curve.

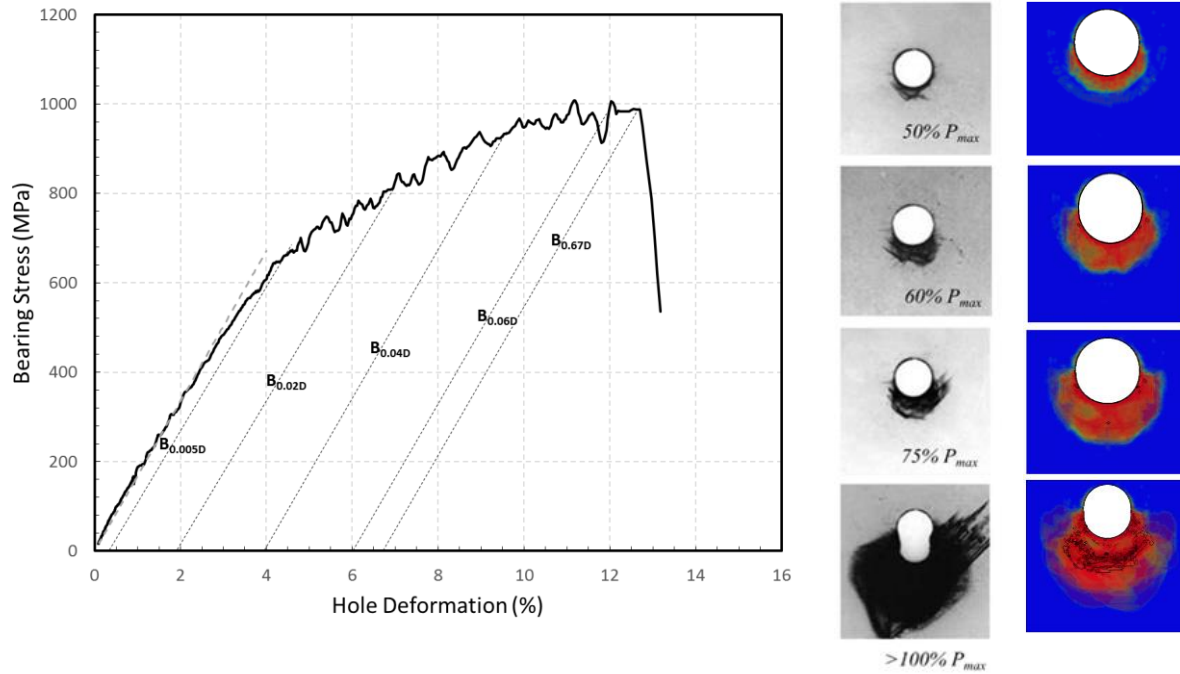


Figure 5. Predicted Bolt Bearing Stress vs. Hole Deformation (left) and qualitative comparison between simulated and experimentally-observed (X-Ray tomography; from [15]) bolt bearing damage at several load levels (right).

In order to study the influence of the bolt clamping pressure on the bearing response, different torque values of 1.3 Nm and 5.4 Nm were simulated. The correlation between experimental and numerical results is shown in Table 1, for different hole deformation values up to ultimate bearing strength. It can be concluded that the application of the appropriate torque value (5.4 Nm) is important to the correct virtual representation of the bolt bearing test.

Table 1. Correlation between experimental and simulation bolt bearing stress results including the influence of application of different bolt torques values.

Bearing hole deformation	Test result [MPa]	Simulation result [MPa]	
		Bolt torque: 1.3Nm	Bolt torque: 5.4Nm
0.005D (0.5%)	747.0	594.7	727.2
0.02D (2%)	894.0	734.6	885.1
0.04D (4%)	975.0	821.0	952.2
0.06D (6%)	989.0	883.8	996.1
Ultimate stress	1006.0	964.4	1009.2

3.3. Low-velocity impact and compression-after-impact

The Virtual Test Lab also incorporates modelling techniques that allow the prediction of LVI damage resistance and CAI strength of unidirectional composite laminates. In the case of LVI, the drop-weight impact test standard ASTM D7136 [16] is simulated for different impact energies, as described in [17], to predict visible and barely visible impact damages (VID and BVID) on composite laminates and their overall impact damage resistance. After the rebound of the impactor and damping of the major specimen vibrations, a simulation step is added to represent the CAI conditions defined by ASTM D7137 [18] until specimen collapse. These simulations allow the prediction of the damage tolerance of the previously impacted laminates.

As an example, the simulation of a 45J LVI test on a 10/80/10 coupon (see section 3.1) made of AS4/8552 plies is illustrated in Figure 6. In general, good correlations are achieved with experimental data with respect to specimen load-displacement behaviour, ply damage, impact footprint, and interface-by-interface delaminations, as demonstrated in [17].

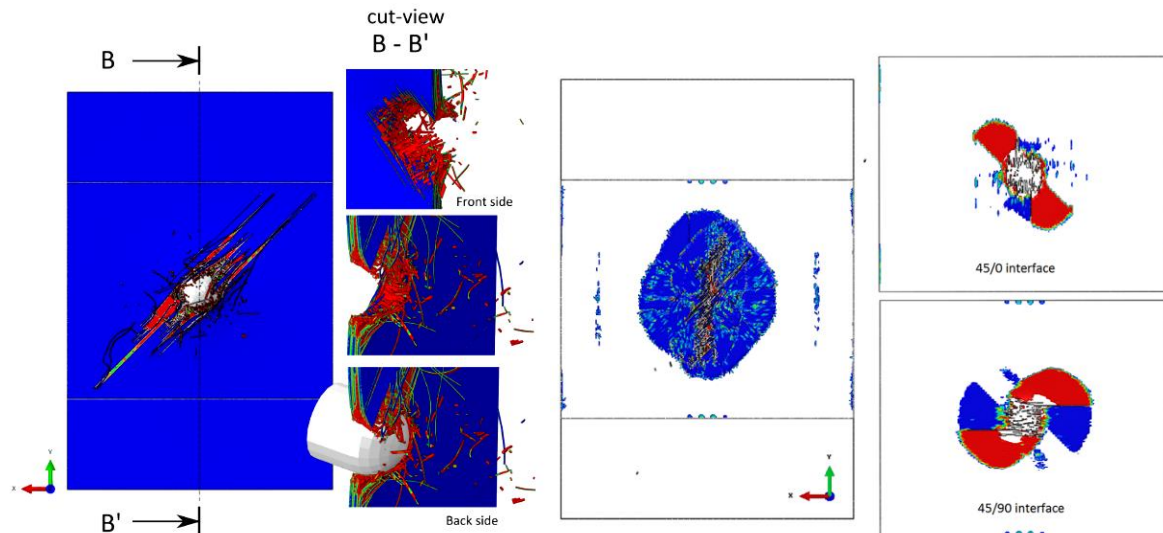


Figure 6. Simulation of 45J LVI on configuration 10/80/10: left) impact dynamics and ply damage; centre) impact footprint; e) delamination at selected interfaces.

The simulation of the CAI test on the 10/80/10 laminate specimen previously impacted at 21J, and showing BVID, is represented in Figure 7. This type of analysis allows the prediction of the residual compressive strength within a margin of accuracy of 20%, and the identification of most important damage mechanisms. In the case of BVID, specimen collapse is driven by the instability and delamination of critical sublaminates.

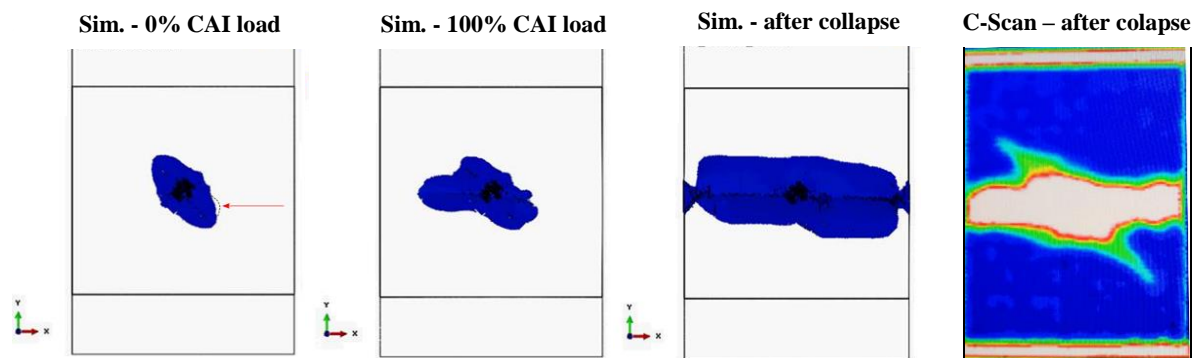


Figure 7. Simulated propagation of delamination at increasing load levels of CAI and comparison with ultrasonic C-Scan data (configuration 10/80/10 impacted at 21J).

4. Conclusions

A reliable Virtual Test Lab has been developed, demonstrating that the sound kinematic simulation of composite damage modes and the accurate prediction of failure loads can be achieved by combining conventional constitutive approaches with appropriate discretization and meshing of ply and interfaces. This computational framework constitutes a powerful tool to aid in the huge effort currently involved in structural design and certification of composite materials and structures in the aeronautical sector [19]. The tool is also promising for screening of a vast range of materials and configurations under general loading conditions. Through this approach, standard experimental tests can be reliably simulated in a computational environment allowing for an effective reduction of time-consuming and costly physical test campaigns. It is foreseen that a hybrid virtual-physical testing approach will provide the means of analyzing a structure by rapid conventional methods supported by simulation and

high-fidelity methods allowed for evaluation of new structural details that would normally require physical testing [20]. The fundamental next steps in development to allow an increased confidence in the virtual test lab include the coupling with process simulation tools in order to account for manufacturing defects and material variability and their effects on structural behaviour. As with experimental results for material certification, simulation results will need to be analysed from a statistical perspective instead of a deterministic one.

Acknowledgments

This research had the support of GKN Aerospace: Fokker through project VIRTEST (Multiscale Virtual Testing of CFRP Samples), of EU's Horizon 2020 Framework Programme for the Clean Sky Joint Technology Initiative 2, through grant agreement n. 686946 (REDISH project), and of AIRBUS SAS by means of project SIMSCREEN (Simulation for Screening Properties of Composite Materials).

References

- [1] ABAQUS v. 6.14 online documentation, Analysis user's manual, SIMULIA Inc., Dassault Systèmes, 2013.
- [2] P. Maimí, P. P. Camanho, J. A. Mayugo, C. G. Dávila, A continuum damage model for composite laminates: Part i - constitutive model, *Mechanics of Materials* 39 (2007) 897-908.
- [3] P. Maimí, P. P. Camanho, J. A. Mayugo, C. G. Dávila, A continuum damage model for composite laminates: Part ii - computational implementation and validation, *Mechanics of Materials* 39 (2007) 909-919.
- [4] W. Ramberg, W. R. Osgood, Description of stress-strain curves by three parameters, National Advisory Committee For Aeronautics (1943). Technical Note No. 902.
- [5] G. Catalanotti, P. P. Camanho, A. T. Marques, Three-dimensional failure criteria for fiber-reinforced laminates, *Composite Structures* 95 (2013) 63-79.
- [6] C. G. Dávila, C. A. Rose, P. P. Camanho, A procedure for superposing linear cohesive laws to represent multiple damage mechanisms in the fracture of composites, *Int. Journal of Fracture* 158 (2009) 211-223.
- [7] M. L. Benzeggagh, M. Kenane, Measurement of mixed-mode delamination fracture toughness of unidirectional glass/epoxy composites with mixed-mode bending apparatus, *Composites Science and Technology* 56 (1996) 439-449.
- [8] O. Falcó, R. L. Ávila, B. Tijs, C.S. Lopes, Modelling and simulation methodology for unidirectional composite laminates in a Virtual Test Lab framework, *Composite Structures*, 190 (2018) 137-159.
- [9] Z. Bažant, B. Oh, Crack band theory for fracture of concrete, *Materials and Structures* 16 (1983) 155-177.
- [10] M. Jirásek, T. Zimmermann, Analysis of rotating crack model, *Journal of Engineering Mechanics* 124 (1998) 842-851.
- [11] NCAMP, Hexcel 8552 AS4 Unidirectional Prepeg Qualification Statical Analysis Report, Technical Report, National Center for Advanced Materials Performance, 2011. CAM-RP-2010-002 May 6, Revision A.
- [12] Liyong Tong, Bearing failure of composite bolted joints with non-uniform bolt-to-washer clearance, *Composites: Part A* 31 (2000) 609-615
- [13] U.A. Khashaba, H.E.M. Sallam, A.E. Al-Shorbagy, M.A. Seif, Effect of washer size and tightening torque on the performance of bolted joints in composite structures, *Composite Structures* 73 (2006) 310-317.
- [14] AITM 1-0009, Airbus Test Method Fibre Reinforced Plastics Determination of Bearing Strength by either Pin or Bolt Bearing Configuration, 2003.
- [15] A. Atlas, C. Soutis Subcritical damage mechanisms of bolted joints in CFRP composite laminates, *Composites: Part B* 54 (2013) 20-27.
- [16] ASTM D7136/D7136M-05. Standard Test Method for Measuring the Damage Resistance of a Fiber-Reinforced Polymer Matrix Composite to a Drop-Weight Impact Event. ASTM International. West Conshohocken PA, USA. 2005.
- [17] C.S. Lopes, S. Sádaba, C. González, J. LLorca, P. P. Camanho, Physically-Sound Simulation of Low-Velocity Impact on Fibre Reinforced Laminates, *Int. Journal of Impact Engineering* 92 (2016) 3-17.
- [18] ASTM D7137/D7137M-05. Standard Test Method for Compressive Residual Strength Properties of Damaged Polymer Matrix Composite Plates. ASTM International. West Conshohocken PA, USA. 2005.
- [19] C.S. Lopes, C. González, O. Falcó, F. Naya, J. Llorca and B. Tijs. Multiscale virtual testing: the roadmap to efficient design of composites for damage resistance and tolerance. *CEAS Aeronautical Journal*, 7(4):607-619, 2016.
- [20] B. Tijs, C.S. Lopes, A. Turon, C. Bisagni, J. Waleson, J.W. van Ingen, S.L. Veldman, Virtual Testing of Thermoplastic Composites: Towards a Hybrid Simulation-Physical Testing Pyramid, ECCM18 - 18th European Conference on Composite Materials, Athens, Greece, June 2018.